Sheath Current Monitoring at HVAC Power Cable Joints Using Fibre-Optic Distributed Acoustic Sensing

Ralf **ALBRECHT**, Sebastian **BOHR**, Jonathan **LUX**, Wieland **HILL**, Gareth **LEES;** AP Sensing GmbH, (Germany),
ralf.albrecht@apsensing.com, sebastian.bohr@apsensing.com, jonathan.lux@apsensing.com,
wieland.hill@apsensing.com, gareth.lees@apsensing.com

Oliver **HEEB**, Ronny **STEINHAUS**; Brugg Cables AG, (Switzerland),

oliver.heeb@bruggcables.com, ronny.steinhaus@bruggcables.com

☐ **Young Researcher** (Proved full-time engineering and science university researchers and Ph.D.students under 35 YO)

ABSTRACT

A new method for permanent sheath current monitoring is introduced, which uses fibre-optic distributed acoustic sensing (DAS). Fully passive current sensors and signal transducers installed at terminations or link boxes can be connected to a fibre which is interrogated by a DAS system. The DAS can detect and localize third party intrusion (TPI), and cable faults as well as the optically transmitted current data from the sensor locations. Function and performance of the sheath current monitoring system are verified by lab investigations and by the results of a field study.

KEYWORDS

Sheath current, optical fibre, distributed acoustic sensing, permanent monitoring, current sensor, insulated power cable, HVAC, cross bonding, link box

INTRODUCTION

Insulated HVAC power cables are increasingly used for transmission and distribution of electrical power because of efficient installation techniques, less effected by environmental influences and no visual impact which increases the public acceptance and results in a high usage in urbanized areas. Cables are more and more operated close to their technical limits due to the increasing share of weather-dependent and variable renewable energy supply [1]. High load operation of cables makes permanent condition monitoring essential, especially if cables are installed in densely populated urban areas. Distributed fibre-optic sensing (DFOS) systems like distributed temperature sensing (DTS) or DAS are meanwhile widely used in power cable monitoring [2, 3] as they can efficiently monitor the entire length of a cable installation by using just ordinary telecommunication fibres, and because they are immune to electromagnetic interference.

DTS measures the temperature of the cable screen and is used in combination with real-time thermal rating (RTTR) for determining conductor temperatures and for predicting the dynamic ampacity of cables [4]. DAS is used for cable fault detection and localization. An analysis of significant factors on cable failures can be found in [5].

In the present paper, we introduce a new method and accessory for DAS that enables permanent monitoring of sheath currents at cable terminations and joints.

Cables in operation carry capacitive and inductive currents in their sheaths. Excessive currents and voltages that could damage the cable or reduce the ampacity are usually avoided by using proper grounding and cross bonding schemes. Sheath current measurements can detect installation failures and material related degradation of the grounding and bonding system caused by environmental influences. They can also be used to reveal unwanted ground contact, for instance by damaged outer jackets or flooded link boxes [6, 7].

Our approach on permanently measuring sheath currents at terminations and link boxes of HVAC cables is based on conventional current transformers (CT's) connected to piezoelectric fibre stretchers that transform the output of the CT into fibre elongation. The fibre stretchers are integrated into the fibre route of a DAS system. A single DAS can measure the currents at multiple locations and cables by analysing the local fibre elongations.

EXPERIMENTAL

The metal sheath of HVAC cables is grounded at the terminations to reduce induced voltages to a safe level [8]. Since induced currents in a both-side grounded sheath could significantly contribute to cable losses and heating, cross bonding of sheaths from different phases is used at link boxes between cable sections to reduce such currents.

Link boxes and terminations are the locations where the sheath current is accessible for measurements, either in individual conductors at terminations or in coaxial cables carrying the sheath currents of two phase cables at link boxes. Our sensor technology can be installed in these locations and used for a permanent measurement and evaluation of currents.

Sensing principle

The schematic setup of a current sensor and transducer is shown in Figure 1. A CT clamped around a coaxial or single conductor cable is used to convert sheath current (primary current I_p) into a secondary current (I_s) signal that is then further converted to a voltage signal by a burden resistor. The voltage drives a piezoelectric fibre stretcher that elongates the optical fibre wound around the piezo. The periodic elongation of the fibre is thus proportional to the sheath current to be measured:

$$\boldsymbol{strain}\ [\boldsymbol{p\epsilon}] \propto \boldsymbol{I_s} \propto \boldsymbol{I_p}. \qquad (1)$$

To avoid overvoltages and the associated damages of the sensor elements in case of excessive primary currents, a transient voltage suppressor (TVS) diode has been installed. The whole sensor-transducer setup works without any external power supply, just based on the energy harvested by the CT. It should be noted that sheath currents of the phase cables are directly measured at the terminations, whereas the coaxial cables at the link boxes allow for measurements of current differences only.

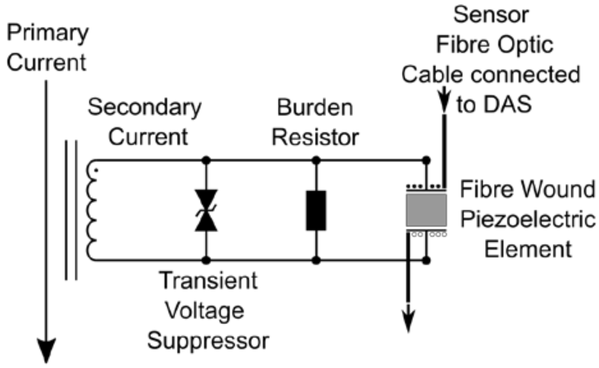

Figure 1: Schematic drawing of the current sensor with all relevant components. The primary current corresponds to the sheath current to be measured and the secondary current is the proportional current generated by the CT. Via the burden resistor, the secondary current is converted into a proportional voltage that drives the piezoelectric element. As a consequence, the attached fibre is elongated.

Multiple current sensors with fibre-optic transducers can be connected to a single telecommunication fibre running along the route of the power cable. A DAS interrogator can then be used to monitor the whole cable route including the current sensors. Fibre outside the transducers is used for traditional DAS applications like TPI and fault detection, whereas the periodic elongation signals from the transducers are used to generate current readings.

Current readings can be efficiently separated from potentially interfering acoustic or vibration signals in the vicinity of the cable because fibre elongations have a periodicity determined by the power grid frequency, which allows narrowband spectral filtering. The readings are also immune to electromagnetic interference because of the fully optical transmission within fibres.

Sensor characteristics

From equation (1), it is obvious that the strain measured by the DAS is proportional to the primary current. However, the DAS as interrogation system can only detect small dynamic strains which limits the frequency and magnitude of the strain signal generated by the piezoelectric fibre stretcher. As a result, our current measurement range is always restricted by the dynamic range of the DAS. To allow for an adjustment of the current range to the interrogator's dynamic range, the resistance of the burden resistor can be adapted.

A DAS interrogator analysing strain quantitatively by measuring phase changes of returning light is used in our investigation. A detailed explanation of the phase extraction of DAS sensors is not within the scope of this paper and can be found elsewhere [9].

Table 1 shows typical sensor accuracies for different current measurement ranges and DAS settings. Note, we specify our current value as effective value ($\mathrm{A_{eff}}$) corresponding to the DC equivalent value. Larger current ranges ($100\ \mathrm{A_{eff}} \rightarrow 275\ \mathrm{A_{eff}}$) interrogated with the same DAS settings lead to a slight reduction of accuracy as a consequence of the higher current range mapped to the same DAS dynamic range. The sampling rate of $10\ \mathrm{kHz}$ corresponds to the DAS pulse rate of the injected light pulses into the fibre and is the limiting factor in terms of total fibre length and frequency bandwidth of transient events. Longer distances between the interrogator and the current sensor require lower pulse rates as shown in set 3. Obviously, the current measurement range must be decreased ($275\ \mathrm{A_{eff}} \rightarrow 225\ \mathrm{A_{eff}}$) to achieve the same accuracy, since in this specific set, the decreased pulse rate ($10\ \mathrm{kHz} \rightarrow 2.5\ \mathrm{kHz}$) also coincides with a lower dynamic range to map the current range.

	Set 1	Set 2	Set 3
Current Range	$100\ \mathrm{A_{eff}}$	$275\ \mathrm{A_{eff}}$	$225\ \mathrm{A_{eff}}$
Meas. Range	10 km	10 km	35 km
1σ Accuracy	< 2.5 %	< 3.1 %	< 3.1 %
Readout Rate	1 s	1 s	1 s
Sampling Rate	10 kHz	10 kHz	2.5 kHz

Table 1: Three individual parameter sets demonstrate the achievable accuracy. Here, the readout rate corresponds to the mean time of the current signal and the sampling rate is equivalent to the pulse rate of the DAS, defining the spectral bandwidth and dynamic range of the measurement.

In brief, our newly developed current sensor features a high accuracy, and allows for long distances between remote sensing locations and the interrogator. In dependence of the requirements, different current measurement ranges and bandwidths can be realized.

Sensor calibration

Since the interrogation system measures strain proportional to the sheath current, a proper calibration factor must be determined. Figure 2 shows the calibration data of three sensors connected to a cable carrying a known current. Here, the sensors are located at fibre positions $1020\ \mathrm{m}$, $1080\ \mathrm{m}$ and $1140\ \mathrm{m}$. The attached section of the fibre within the piezoelectric element of each sensor has a length of $40\ \mathrm{m}$. In between each two sensors, $20\ \mathrm{m}$ of non-attached fibre is added to separate the individual current transducers and to avoid interference of different signals.

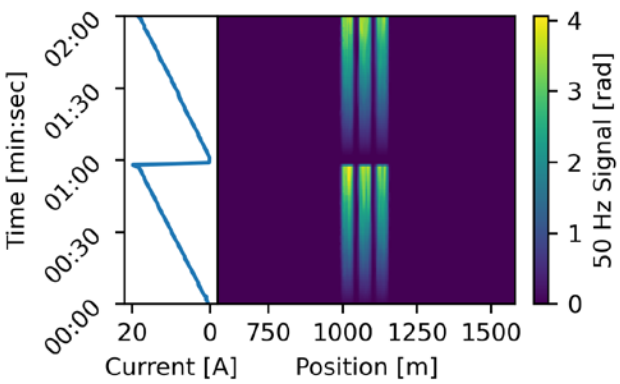

Figure 2: Sensor calibration data for three fibre-optic current sensors measuring the same current. Left: Applied effective current at 50 Hz. Right: Proportional phase measured by the DAS interrogator. Note that the strain data shown is frequency filtered at 50 Hz to reduce noise and to suppress other interfering signals.

On the left side of this figure, the generated $50\ \mathrm{Hz}$

alternating current with increasing amplitude is illustrated. The proportional strain magnitude measured along the fibre segment between 580 m and 1580 m is depicted on the right side. The measured phase signal is converted to the frequency-domain through Fourier transforms. Subsequently, we can analyze the frequencies of interest, for instance 50 Hz and higher harmonics. In order to increase the accuracy, we average the signal of the spatial channels of the contact portion and calculate the frequency spectrum for a minimum phase time series of 1 s.

Discussion of use cases

According to the sensor characteristics, we demonstrate that our newly developed point current sensor features a high accuracy, allows an installation in remote locations several tens of kilometers away from the interrogation system and does not require any power supply. For the purpose of measuring three phase alternating currents, our hardware device consists of three sensors in a waterproof enclosure as depicted in Figure 3(a). With regard to installations in harsh environments such as pits or manholes where the sensor is exposed to the elements, it is necessary to characterize the temperature stability.

The quantitative DAS based on phase-sensitive optical time-domain reflectometry (Φ-OTDR) is insensitive to temperature fluctuations of the sensor fibre since they typically appear in the mHz-range and have no impact on our signal frequencies ≥ 50 Hz. On the other hand, the capacitance of the piezoelectric element shows a slight thermal sensitivity which results in a temperature dependent strain sensitivity. However, temperature cycling tests reveal that this material property can be neglected as we observe a sensitivity on the order of 0.1 % per °C only.

If a suitable telecom cable for DAS runs close to the power cable, our sensor allows for subsequent installation. Even an installation during cable operation is possible, as the CT is non-invasive and the primary and secondary circuits are galvanically isolated. All things considered, our solution is well suited for on-line monitoring of cable sheaths.

Despite the fact that grounding systems like single point or cross bonding are designed to minimize the sheath currents, it is not possible to eliminate the sheath currents completely. Inductive circulating currents on cable sheaths can be generated as a consequence of lengths differences between minor sections and are directly proportional to the applied load. Capacitive currents generated by loading and unloading the capacitance between the conductors and the metal sheaths, respectively the metal sheaths and ground cannot be suppressed and are always present when the cable is operating. As a consequence, it can be derived that the sheath currents are sensitive to changes in the different capacitances, thus sensitive to the insulation between the conductor/metal sheath and metal sheath/ground. As measured and analyzed in [10], permanent monitoring is able to detect problems with the cable jacket implying a loss of insulation and a resulting increase of the sheath current of the corresponding phase. Failure of the sheath voltage limiter (SVL) inside link boxes of cross bonding systems or in between the open end of metal sheath and the local earth link in single point bonding systems results in an additional ground point leading to circulating sheath currents proportional to the load. In case of theft of the ground cable at the beginning or the end of a major section, the accumulated sheath currents at this location cancel out and thus events can be detected as well. Other problems such as flooded link boxes, open circuit faults in grounding points, or insulation breakdowns in joints have been theoretically investigated [6] and should be distinguishably detectable.

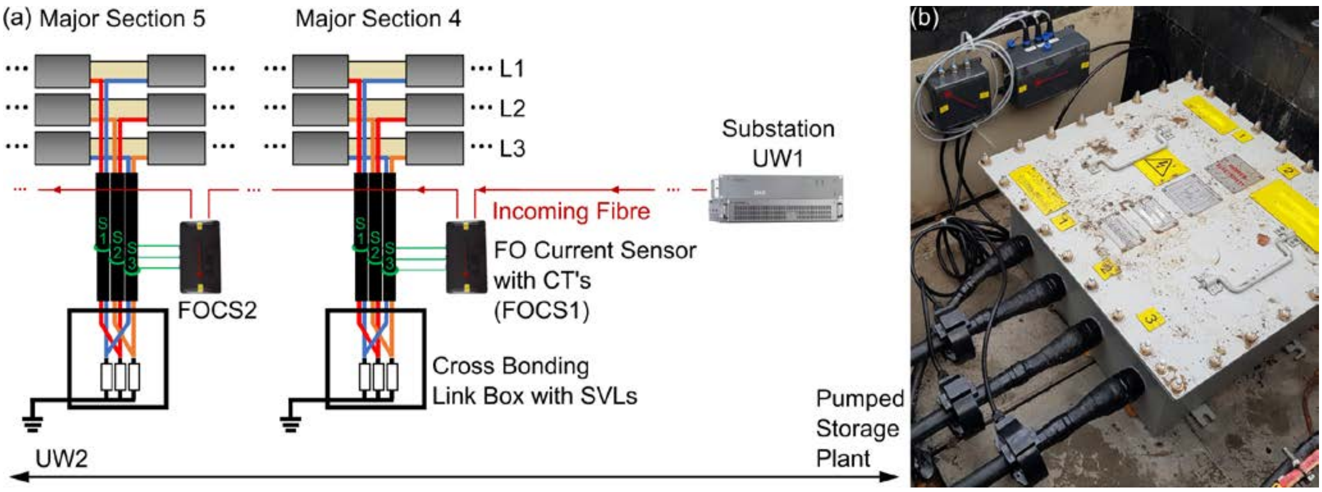

Figure 3: (a) Schematic illustration of the DAS and current sensor installation. The sensors are installed in manholes at two different major sections and spliced to the DAS sensor fibre. (b) Picture of the installed FO current sensor with the CT's clamped around the coaxial cables leading into the cross bonding link box.

CASE STUDY – 110 KV LINE

Following the verification and specification of the current sensor under laboratory conditions, we installed the sheath current monitoring (SCM) system under real environmental conditions on a 110 kV HVAC power cable in sectional cross bonding configuration [8]. The installation took place in August 2022 and has been recording sheath currents ever since.

Description of the cable structure and sensor installation

The monitored underground cable has an overall length of 32 km with 35 cable joints and is sectionized into 5 major sections with lengths of ~5450 m. Furthermore, the typical minor section length is 1800 m long. In major section 4, the minor section lengths in a consecutive order are $1790\ \mathrm{m}$, $1850\ \mathrm{m}$, $1815\ \mathrm{m}$ indicating an imbalance of $3\ \%$. The neighboring major section 5 consists of minor sections with lengths of $1835\ \mathrm{m}$, $1800\ \mathrm{m}$, and $1875\ \mathrm{m}$ indicating an imbalance of $4\ \%$. Both sections have been explicitly mentioned because we installed our sensors to measure the sheath currents at link boxes there. From the imbalances we expect to measure comparable signals in different locations with a weak dependency on the load.

The cables used consist of aluminium conductors with a cross section of $800\ \mathrm{mm}^2$ and a XLPE insulation to the metal sheath. In addition, the sheath wires in terminations and cross bonding or grounding boxes have an effective conductor cross section of $57\ \mathrm{mm}^2$. Regarding these specifications, the cables are rated for a maximum ampacity of $525\ \mathrm{A_{eff}}$.

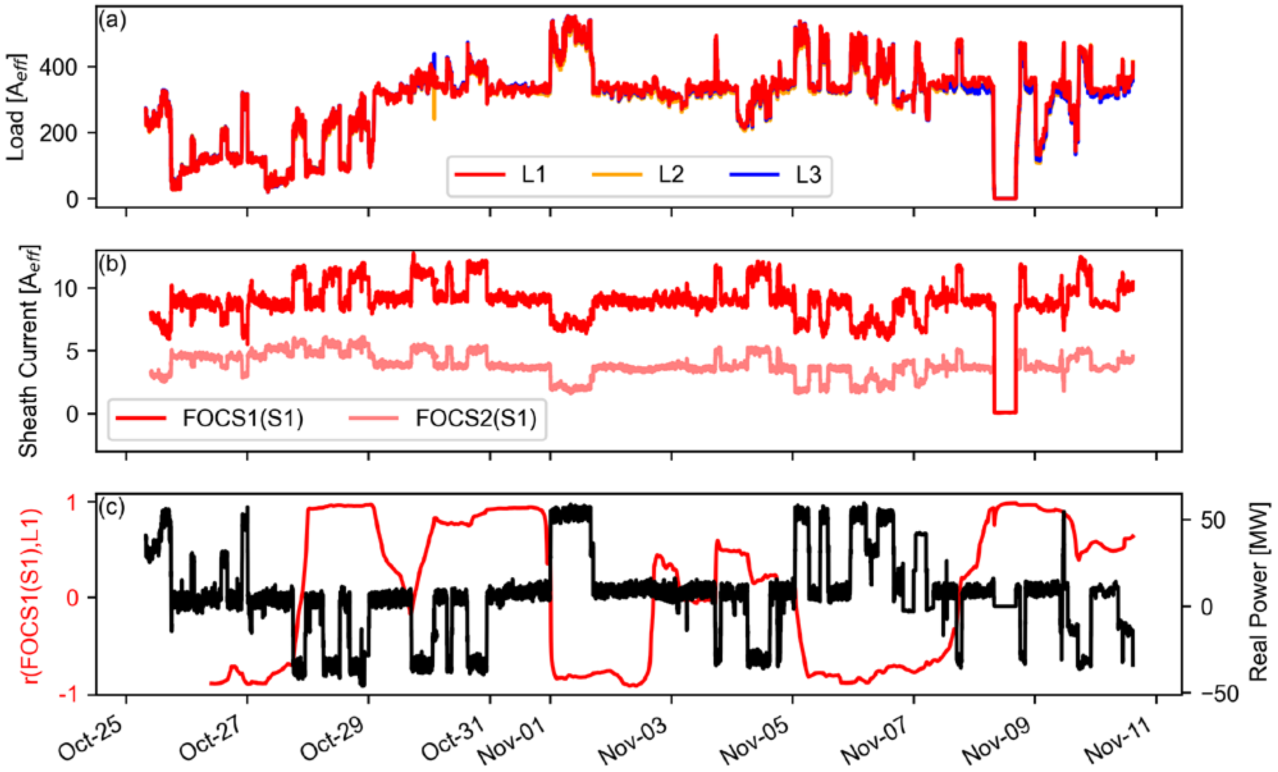

Figure 4: History of measured sheath currents for the period October 25 to November 11. (a) Load data of all 3 lines for the given period. (b) Corresponding measured sheath currents on major section 4 (dark red) and 5 (light red). Here, we only show the sensors S1 connected to L1 in order to ensure a clear presentation. (c) Real power of the cable (black) and Pearson correlation coefficient r of FOCS1(S1) and the load of L1 (red).

A schematic overview of the power cable along with the installed fibre optics is depicted in Figure 3(a). The DAS is located in substation UW1 with a fibre optic sensor cable connected to it directing to substation UW2. At a distance of $20.8\ \mathrm{km}$, our fibre optic current sensor (FOCS1) is installed at a cross bonding link box on major section 4. Another FOCS2 is installed on major section 5 at a distance of $28.1\ \mathrm{km}$ from the interrogator. As indicated by the arrow in the bottom of this schematic, a pumped storage plant is connected to the cable in the immediate vicinity to UW1. Alongside two induction motors, a dynamic power factor correction in order to control the reactive power generated is installed. The substation UW2 is connected to the $380\ \mathrm{kV}$ transmission grid and features a dynamic power factor correction to stabilize the grid voltage. Figure 3(b) illustrates the installed FOCS inside the manhole. As one can see, the CT's (S1,S2,S3) are clamped around coaxial cables connected to the link box. The installed sensor S_i measures the following sheath currents I_s:

$$S1 = I_s(L1) - I_s(L3), \qquad (2)$$

$$S2 = I_s(L2) - I_s(L1), \qquad (3)$$

$$S3 = I_s(L3) - I_s(L2). \qquad (4)$$

From equation (2) to (4), one can see that our sensors measure the differential currents of two sheaths.

Evaluation of measurement data

Figure 4 illustrates the measurement results of the FOCS's for a period of 18 days. In the top panel the cable loads L1-3 are displayed. Here, one can see that the entire ampacity up to $525\ \mathrm{A_{eff}}$ is used. In the middle panel, the measured sheath currents of S1 in both locations are shown. For a clear representation, we only visualize one sensor, but S2 and S3 shows a similar behavior in dependence of their differential current components. The difference in the overall offset between FOCS1 and FOCS2 is related to the power factor correction in UW2. FOCS2 is measuring currents in the closest location to the compensation. For this reason, the overall offset is much lower as for FOCS1 on major section 4. Note, the mean value of FOCS1 is $\sim 10\ \mathrm{A_{eff}}$, whereas the measured mean value of FOCS2 corresponds to $\sim 5\ \mathrm{A_{eff}}$. Both values are within the normal operating range of power cables in a cross bonding configuration indicating a proper condition of the cable. On November 8, the cable operation was interrupted due to scheduled maintenance work. As a result, the load of all phases is $0\ \mathrm{A_{eff}}$ and so do the associated sheath currents.

The bottom panel illustrates the real power (black line) carried by the cable. Here, the sign indicates the direction of the power. A positive sign corresponds to a pumping and storing energy, whereas a negative sign is associated with the generator operation mode of the pumped storage plant. Note, the weak correlation between the load and real power arises from the dynamic power factor corrections. For a better understanding of the power data, it should be mentioned that there are a total of two generators with $25\ \mathrm{MVA}$ each installed in the hydropower plant. The sudden increase and decrease in power corresponds to the motors being switched on and off ($2 \times 25\ \mathrm{MVA} = 50\ \mathrm{MVA}$).

The red line in the bottom panel of Figure 4 shows the 24-hour Pearson correlation coefficient of load and sheath currents. As predicted from the small imbalances of the minor section lengths, we observe a weak coupling between the sheath currents and their loads. However, we expect these currents to be highly correlated and they are. We observe a strong correlation, when the pumped storage plant is in generator operation, and strong anticorrelation during pumping, as the current is flowing in the opposite direction, which is not captured in the effective load currents. This behavior can be explained as follows, the amplitudes of the capacitive currents $I_c(L_i)$ on each phase are constant for a constant line voltage amplitude which is always given. Therefore, FOCS1(S1) measures in positive direction $S1 = I_c(L1) - I_c(L3) + I_i(|L1|) - I_i(|L3|) = I_c + \Delta I_i$. Here, $I_i(L_i)$ corresponds to the inductive currents coupled into the sheath. The resultant correlation is strongly positive.

Obviously, inductive currents are highly dependent on the direction of the conductor current and the associated magnetic field direction. For this reason, FOCS1(S1) measures in negative direction $S1 = I_c + I_i(|L3|) - I_i(|L1|) = I_c - \Delta I_i$, which results into a strong anticorrelation. At times, when the level of power factor correction is switched, the correlation is weakened (e.g. on October 29).

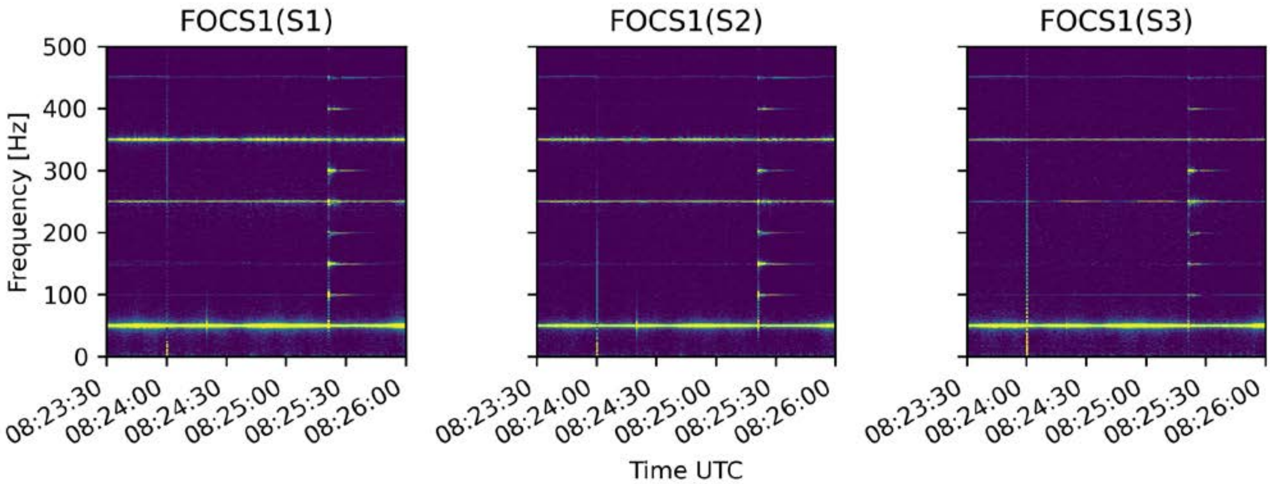

Figure 5: Spectral response of a large consumer connected to the power cable. Two broad band events are visible at 8:24:00 and 8:25:20 corresponding to dynamic power factor correction. The power at 50 Hz exceeds the color scale to allow better visibility at other frequencies.

Figure 5 shows the spectrogram of the recorded current in each sensor of FOCS1 for a 2:30 minute time window, illustrating the frequencies present at each one second interval. The expected $50\ \mathrm{Hz}$ signal corresponding to the power grid frequency is clearly visible at the bottom and exceeds the chosen color scale to allow for better visibility of weaker components. In the rest of the spectrum, higher harmonics of the base signal at multiples of $50\ \mathrm{Hz}$ are visible as horizontal lines across the full time window, with 250 and $350\ \mathrm{Hz}$ being stronger than other harmonics.

At 8:24:00 and 8:25:20, broad band signals are visible on all three sensors for one second, and the later event strengthens the harmonics for about 20 seconds. Sudden events, like connecting or disconnecting large consumers, can cause inrush currents leading to a step in the currents and these steps have a very broad spectral response as observed. In the present case, the dynamic power factor compensation was switched on and caused the visible events. As the compensation is connected to all three phases, all sensors, also at FOCS2, detected this event and show very similar responses. Other sudden events, caused by faults or intrusion, would create a similar spectral response. But as these events would not occur on all three cables, the response would only be seen on the sensors connected to the corresponding sheath, but not on the other sensors, making it possible to determine the affected cable. Together with TPI detection of the DAS, this can be used to detect if a TPI event affected the power cable.

SUMMARY AND OUTLOOK

A new method for permanent monitoring of sheath currents at HVAC cable terminations and link boxes has been developed. It is based on fully passive current sensors and transducers without need for any electrical power supply in the field. Data is transmitted via optical fibres to a DAS system, which can monitor currents at multiple terminations and link boxes in combination with other DAS applications such as TPI or fault detection.

The performance of the new sheath current monitoring solution has been demonstrated in the lab and in a field study.

Sheath currents depend in a complex way on cable design and load, cable installation, bonding scheme and different defects on cables or link boxes. It is therefore not easy to develop a precise model for sheath currents and their dependence on defects. Nevertheless, several defects are expected to change currents in a significant way and should be detectable by comparing the present currents with a history of currents under the same load conditions. Further investigations are required to determine the sensitivy of sheath currents to different failure scenarios.

Acknowledgments

We are indebted to the Engadiner Kraftwerke AG for their generous support and facilitating this case study. We thank you for the access on site and valuable discussions about the measurement results.

REFERENCES

[1] «European Grid Perspectives,» Renewables Grid Initiative, Berlin, 2018.

[2] G. Cedilinik, G. Lees, P. E. Schmidt, S. Herstrom et G. T., «Ultra-Long Reach Fiber Distributed Acoustic Sensing for Power Cable Monitoring,» chez *JiCable*, 2019.

[3] O. Hobberstad, T. Lucignano, J. Lux et W. Sfar Zaoui, «Offshore Power Cable Mapping and Exposure Identification based on the DTS and DAS Technologies,» chez *Tekna Seabed Mapping and Inspection*, Geilo, 2023.

[4] A. Farahani, G. J. Anders, E. Bic et U. Keppler, «A new approach for estimation of the dynamic thermal rating model parameters based on the IEC standard,» chez *JiCable*, Versailles, 2015.

[5] Z. Tang, C. Zhou, W. Jiang, W. Zhou, X. Jing, J. Yu, B. Alkali et B. Sheng, «Analysis of Significant Factors on Cable Failure Using the Cox Proportional Hazard Model,» *IEEE Transactions on Power Delivery,* vol. 29, pp. 951-957, April 2014.

[6] X. Dong, Y. Yang, C. Zhou et D. M. Hepburn, «Online Monitoring and Diagnosis of HV Cable Faults by Sheath System Currents,» *IEEE Transactions on Power Delivery,* pp. 2281-2290, 2017.

[7] B. Zhu, X. Yu, L. Tian et X. Wei, «Insulation Monitoring and Diagnosis of Faults in Cross-Bonded Cables Based on the Resistive Current and Sheath Current,» *IEEE Access,* vol. 10, pp. 46057-46066, April 2022.

[8] «TB 797 - Sheath bonding systems of AC transmission cables - Design, testing, and maintenance,» CIGRE, 2020.

[9] A. H. Hartog, An Introduction to Distributed Optical Fibre Sensors, 1 éd., Boca Raton: CRC Presss, 2017, p. 472.

[10] A. Burgos, G. Donoso et B. Garcia, «Sheath currents monitoring in high voltage isolated cables,» chez *Cigre B1-209*, Paris, 2016.